Enzymatic Synthesis of Amorphous Calcium Phosphate−Chitosan Nanocomposites and Their Processing into Hierarchical Structures

María C. Gutiérrez, Matías Jobbágy, María L. Ferrer, and Francisco del Monte*

Instituto de Ciencia de Materiales de Madrid-ICMM, Consejo Superior de Investigaciones Científicas-CSIC, Cantoblanco, 28049 Madrid, Spain

Received July 25, 2007
Revised Manuscript Received November 5, 2007

The requirements for the production of suitable supports for the growth of cells and tissues involve the use of biocompatible and/or biodegradable materials and the processing of the components into a porous matrix of adequate morphology. The nature of the materials most widely used for these purposes is organic (e.g., polymers),[1–4] albeit materials of different nature (e.g., ceramics and carbons meshes, among others) have also been prepared with morphologies suitable for cell growth.[5–7] Materials like hydroxyapatite (HA)[8] and chitosan (CHI)[9] are being widely employed to develop a single three-dimensional (3D) porous structure that combines a mechanical support resembling the subchondral bone (bone-like layer), while also providing a chondrogenic support in the top for the repairing of cartilage (cartilage-like layer).[10] Lately, the use of organic–inorganic composite materials is attracting even increased attention. However, the development of suitable hybrid materials for tissue engineering still requires of further improvement to tailor both the length scale at the organic–inorganic interface and the composition. Controlling the length scale at the organic–inorganic interface within the nanometer range produces a wealth of both novel structural features and enhanced properties arising from the synergistic interaction of the individual constituents, that is, a consequence of the strong mechanical interface between mineral substrate and polymer matrix.[11,12] In regards to the nanocomposite composition, those nanocomposites based on nanoparticles of amorphous calcium phosphates (ACP) would be of greater interest than those based on nanocrystalline HA given that the ultimate formation of bone tissue requires of dissolution of calcium phosphate precursor and subsequent recrystallization which eventually is favored for ACP.[13]

Scheme 1

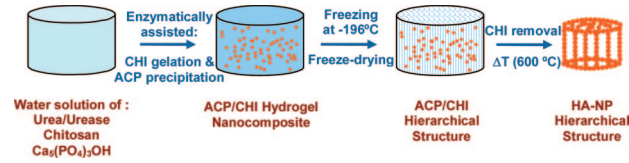

Biomineralization offers the opportunity to produce highly organized nanocomposite structures, controlling specific architectures over extended length scales for a wide range of compositions.[14] Enzymatically assisted routes offer the possibility to synthesize a number of materials with excellent control of the structural organization.[15] In particular, HA precursors and different calcium carbonate precipitates could be obtained in solutions by enzyme-catalyzed decomposition of urea by urease.[16] Furthermore, the gradual generation of base provided by urea hydrolysis has recently been used for the preparation of monolithic and homogeneous chitosan hydrogels.[17] The homogeneous pH modulation besides the low temperature used for urea hydrolysis allows for the achievement of CHI hydrogels with a homogeneous 3D network structure with biotechnological performance superior to that of chitosan solutions gelled by neutralization with alkaline solutions, gaseous NH_3, or dialysis.[18]

Herein, we applied the urease assisted hydrolysis of urea for the preparation of nanocomposites as a result of the simultaneous precipitation of calcium phosphate and CHI gelation (Scheme 1). The base generated by urea hydrolysis promoted both CHI gelation and calcium phosphate precipitation at biological temperatures (∼37 °C). Otherwise (e.g.,

* To whom correspondence should be addressed. E-mail: delmonte@icmm.csic.es.

(1) Yang, J.; Webb, A. R.; Ameer, G. A. *Adv. Mater.* **2004**, *16*, 511.
(2) Stachowiak, A. N.; Bershteyn, A.; Tzatzalos, E.; Irvine, D. J. *Adv. Mater.* **2005**, *17*, 399.
(3) Zhang, Y.; Wang, S.; Eghtedari, M.; Motamedi, M.; Kotov, N. A. *Adv. Funct. Mater.* **2005**, *15*, 725.
(4) Dankars, P. Y. W.; Harmsen, M. C.; Brouwer, L. A.; Van Luyn, M. J. A.; Meijer, E. W. *Nat. Mater.* **2005**, *4*, 568–574.
(5) Mann, S. *Angew. Chem., Int. Ed.* **2000**, *39*, 3392–3406.
(6) Sanchez, C.; Arribart, H.; Giraud-Guille, M. M. *Nat. Mater.* **2005**, *4*, 277.
(7) Correa-Duarte, M. A.; Wagner, N.; Rojas-Chapana, J.; Morsczeck, C.; Thie, M.; Giersig, M. *Nano Lett.* **2004**, *4*, 2233–36.
(8) Kotobuki, N.; Ioku, K.; Kawagoe, D.; Fujimori, H.; Goto, S.; Ohgushi, H. *Biomaterials* **2005**, *26*, 779–785.
(9) Di Martino, A.; Sittinger, M.; Risbud, M. V. *Biomaterials* **2005**, *26*, 5983–5990.
(10) Gao, J.; Dennis, J. E.; Solchaga, L. A.; Goldberg, V. M.; Caplan, A. I. *Tissue Eng.* **2002**, *8*, 827–837.
(11) Tai, K.; Ulm, F.-J.; Ortiz, C. *Nano Lett.* **2006**, *6*, 2520–2525.
(12) (a) Sanchez, C.; Julian, B.; Belleville, P.; Popall, M. *J. Mater. Chem* **2003**, *15*, 3559–3592. (b) Mammeri, F.; Le Bourhis, E.; Rozes, L.; Sanchez, C. *J. Mater. Chem.* **2003**, *15*, 3787–3811.
(13) (a) Webster, T. J.; Ergun, C.; Doremus, R. H.; Siegel, R. W.; Bizios, R. *Biomaterials* **2001**, *22*, 1803–10. (b) Xua, J. L.; Khora, K. A.; Dongb, Z. L.; Guc, Y. W.; Kumarc, R.; Cheang, P. *Mater. Sci. Eng., A* **2004**, *374*, 101–108. (c) Chou, Y.-F.; Chiou, W.-A.; Xu, Y.; Dunn, J. C. Y.; Wu, B. M. *Biomaterials* **2004**, *25*, 5323–5331.
(14) (a) Bigi, A.; Boanini, E.; Walsh, D.; Mann, S. *Angew. Chem., Int. Ed.* **2002**, *41*, 2163–2166. (b) Sanchez, C.; Arribart, H.; Guille, M. M. G. *Nat. Mater.* **2005**, *4*, 277–288.
(15) (a) Zheng, T.; Zhan, J.; Pang, J.; Tan, G. S.; He, J.; McPherson, G. L.; Lu, Y.; John, V. T. *Adv. Mater.* **2006**, *18*, 2735–2738. (b) Zayats, M.; Baron, R.; Popov, I.; Willner, I. *Nano Lett.* **2005**, *5*, 21–25.
(16) (a) Sondi, I.; Matijevic, E. *J. Colloid Interface Sci.* **2001**, *238*, 208–214. (b) Sondi, I.; Matijevicì, E. *Chem. Mater.* **2003**, *15*, 1322–1326.
(17) Chenite, A.; Gori, S.; Shive, M.; Desrosiers, E.; Buschmann, M. D. *Carbohyd. Polym.* **2006**, *64*, 419–424.
(18) (a) Cairns, P.; Miles, M. J.; Morris, V. J.; Ridout, M. J.; Brownsey, G. J.; Winter, W. T. *Carbohyd. Res.* **1992**, *235*, 23–28. (b) Montembeault, A.; Viton, C.; Domard, A. *Biomacromolecules* **2005**, *6*, 653–662. (c) Hu, Q.; Li, B.; Wang, M.; Shen, J. *Biomaterials* **2004**, *25*, 779–785. (d) Li, J.; Chen, Y.; Yin, Y.; Yao, F.; Yao, K. *Biomaterials* **2007**, *28*, 781–790. (e) Kong, L.; Gao, Y.; Lu, G.; Gong, Y.; Zhao, N.; Zhang, X. *Eur. Polym. J.* **2006**, *423*, 171–3179. (f) Wei, G.; Ma, P. X. *Biomaterials* **2004**, *25*, 4749–4757. (g) Shen, X.; Tong, H.; Jiang, T; Zhu, Z.; Wan, P.; Hu, J.; Hu, Q.; Li, B.; Wang, M.; Shen, J. *Compos. Sci. Technol.* **2007**, *67*, 2238–2245.

10.1021/cm7020164 CCC: $40.75
Published on Web 12/06/2007

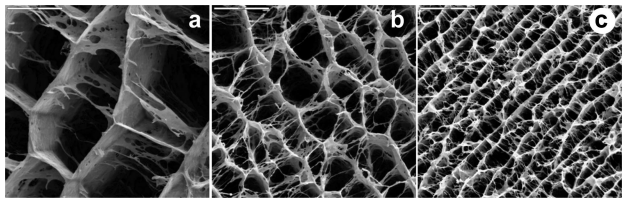

Figure 1. SEM micrographs of different hybrid hierarchical structures resulting from freezing hydrogel nanocomposites, with identical CHI and calcium phosphate composition (93.25 and 6.75 wt %, respectively) at different rates: (a) 0.7 mm/min, (b) 2.7 mm/min, and (c) 5.7 mm/min. Bars are 50 μm.

urea hydrolysis by thermal decomposition at 90 °C), CHI would undergo partial decomposition.[19] Macroporous hierarchical structures were obtained by a cryogenic process[20] (so-called ISISA, ice segregation induced self-assembly)[21] that is simply based on the unidirectional freezing (at −196 °C) of the hydrogel nanocomposite. Upon freezing, the ice formation (hexagonal form) causes every solute originally dissolved/dispersed in the hydrogel to be segregated from the ice phase. After freeze-drying, the resulting hierarchical structures consist of well aligned micrometer-sized pores in the freezing direction corresponding to the empty areas where ice crystals originally resided, being the macrostructure supported by the matter (e.g., calcium phosphate nanoparticles dispersed within CHI matrix) accumulated between adjacent ice crystals. Figure 1 shows the porous channels of up to 90 μm (Figure 1a,b,c) that can be simply obtained by using different freezing rates in the application of the ISISA process to the hybrid hydrogel. The hybrid nature of the hierarchical structure was corroborated by TG/DTA/DSC experiments (see Supporting Information). The porosity of the hierarchical structure was approximately 85%, no matter the freezing rate used for preparation.

The character of the calcium phosphate embedded within the CHI network as HA precursor was confirmed by calcination (at 600 °C) of a monolithic portion of the hybrid hierarchical structure. Actually, novel porous ceramic materials have been described via calcination of their hybrid counterparts.[22] The calcined hierarchical structure was composed of HA nanocrystals (HA-NP), as revealed by the XRD pattern (see Supporting Information). TEM micrographs confirm the formation of clusters of crystalline nanoparticles of approximately 40 nm (Figure 2a). The average particle size of HA-NP calculated from the broadening of different diffraction peaks (002 and 222) using Scherrer's equation was in good agreement with the mean particle sizes observed in TEM micrographs (ca. 45 nm). HRTEM (Figure 2b) shows the interplanar distance of nanocrystalline HA along the [002] zone axis (e.g., 0.3 nm). Interestingly, the calcined hierarchical structure kept both the monolithic shape and the macroporous structure (partially sintered) of the hybrid one (not shown). SEM micrographs (Figure 2c,d) revealed a microsponge-like morphology[23] built of the above-described HA nanocrystalline aggregates. Calibrated energy dispersion X-ray spectroscopy (EDS) analysis performed over the structure of any of the hierarchical structures revealed a Ca/P ratio of 1.65, in good agreement with that of HA (see Supporting Information).[24]

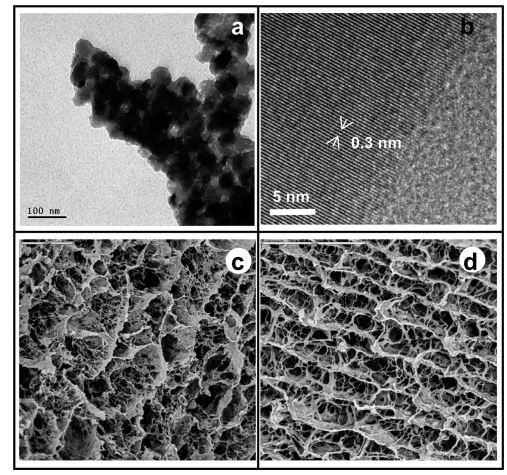

Figure 2. TEM (a) and HR-TEM (b, along [002] zone axis) micrographs of HA crystalline aggregates forming the HA−NP hierarchical structures. Bars are 100 and 5 nm, respectively. SEM micrographs of HA−NP hierarchical structures resulting from calcinations of ACP/CHI hybrid hierarchical structures ISISA processed at freezing rates of 0.7 mm/min (c) and 5.7 mm/min (d). Bars are 20 μm.

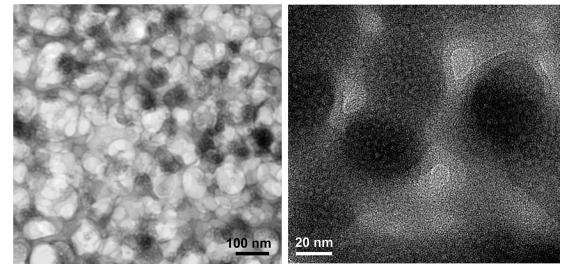

Figure 3. TEM (left) and HR-TEM (right) micrographs of ACP nanoclusters forming the ACP/CHI hierarchical structure. Bars are 100 and 20 nm, respectively.

The question that arises is the nature of the precipitate of calcium phosphate entrapped within the hierarchical structure before calcination. XRD of hybrid hierarchical structure did not exhibit any characteristic diffraction for crystalline HA (see Supporting Information). TEM micrographs (Figure 3) of hybrid hierarchical structure revealed spherical particles of granular aspect, typical of hydrated amorphous calcium phosphate (ACP); that is, $Ca_9(PO_4)_6$ clusters of diameter

(19) Huang, H.; Yuan, Q.; Yang, X. *J. Colloid Interface Sci.* **2005**, *282*, 26–31.
(20) (a) Kuberka, M.; von Heimburg, D; Heschel, I.; Pallua, N.; Glasmacher, B.; Rau, G. *Int. J. Artif. Organs* **2002**, *25* (7), 684. (b) Kuberka, M.; von Heimburg, D.; Schoof, H.; Heschel, I.; Rau, G. *Int. J. Artif. Organs* **2002**, *25* (1), 67–73. (c) Noah, E. M.; Chen, J.; Jiao, X.; Heschel, I.; Pallua, N. *Biomaterials* **2002**, *23* (14), 2855–2861.
(21) (a) Mukai, S. R.; Nishihara, H.; Tamon, H. *Chem. Commun.* **2004**, 874. (b) Gutierrez, M. C.; Hortigüela, M. J.; Amarilla, J. M.; Jimenez, R.; Ferrer, M. L.; del Monte, F. *J. Phys. Chem. C* **2007**, *111*, 5557 and references there in. (c) Gutierrez, M. C.; Garcia-Carvajal, Z.; Hortigüela, M. J.; Yuste, L.; Rojo, F.; Ferrer, M. L.; del Monte, F. *J. Mater. Chem.* **2007**, *17* (29), 2992–2995. (d) Gutierrez, M. C.; Garcia-Carvajal, Z.; Yuste, L.; Rojo, F.; Ferrer, M. L.; del Monte, F. *Adv. Funct. Mater.* **2007** (DOI: 10.1002/adfm200700093). (e) Abarrategui, A.; Gutierrez, M. C.; Moreno-Vicente, C.; Hortigüela, M. J.; Ramos, V.; Lopez-Lacomba, J. L.; Ferrer, M. L.; del Monte, F. *Biomaterials* **2008**, *29*, 94–102.
(22) Ray, S. S.; Okamoto, K.; Yamada, K.; Okamoto, M. *Nano Lett.* **2002**, *2*, 423–425.
(23) Walsh, D.; Lebeau, B.; Mann, S. *Adv. Mater.* **1999**, *11*, 324–328.
(24) (a) Zhang, R.; Ma, P. X. *J. Biomed. Mater. Res.* **1999**, *45*, 285–293. (b) Melde, B. J.; Stein, A. *Chem. Mater.* **2002**, *14*, 3326–3331. (c) Song, J.; Malathong, V.; Bertozzi, C. R. *J. Am. Chem. Soc.* **2005**, *127*, 3366–3372.

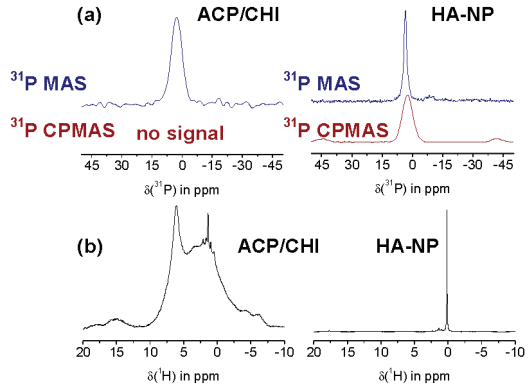

Figure 4. (a) ^{31}P MAS (blue line) and ^{31}P CP MAS (red line) and (b) ^{1}H NMR spectra of ACP/CHI (left column) and HA−NP (right column) hierarchical structures.

approximately 1.0 nm, which pack randomly with respect to each other, forming large 30–50 nm spheres with tightly held water residing within the interstices between clusters.[25] Calibrated energy dispersion X-ray spectroscopy (EDS) analysis performed over the structure of the noncalcined hierarchical structure revealed a Ca/P ratio of 1.5, in good agreement with that of ACP (see Supporting Information). To further corroborate the presence of ACP nanoparticles (ACP−NP) at the hybrid hierarchical structure, we performed ^{31}P and ^{1}H NMR spectroscopy of ACP/CHI and HA−NP hierarchical structures (Figure 4). The isotropic ^{31}P chemical shifts (ppm) measured in MAS NMR experiments were 2.8 and 3.4, respectively (Figure 4a). The ACP line width was 7 ppm, compared to 1.6 ppm for HA, in good agreement with the amorphous character of ACP.[26] The proton coupling (e.g., CP MAS) of ACP completely suppressed the ^{31}P signal after 2 ms of dipolar coupling[26b] which was a predictable consequence of the structural model, that is, absence of protons in the molecular structure and just interstitial water between clusters. The band at ca. 6.5 ppm shown in Figure 4b (e.g., ^{1}H spectrum of the ACP/CHI hierarchical structure) corroborates this issue. Meanwhile the CP MAS spectrum of the HA-NP hierarchical structure reflected the typical features of nanocrystalline hydroxyapatite, that is, appearance of side bands and spectral shift (−0.5 ppm) of the main band, as compared to that of the MAS spectrum.[26c] Moreover, the ^{1}H spectrum of the HA-NP hierarchical structure shown in Figure 4b exhibited a narrow band at approximately 0 ppm ascribed to OH groups of crystalline hydroxyapatite, $Ca_{10}(PO_4)_6(OH)_2$.[26c]

The enzymatic formation of ACP−NP was also confirmed in solution, albeit in this case, the reaction had to be conducted at 0 °C and stopped before the pH rises to 6.5.[18c] Otherwise, crystalline HA was obtained (see TEM micrographs in Supporting Information). However, the pH reached at the CHI hydrogel was 8, and the reaction took place at 37 °C, both features well above those required for achievement of ACP in solution. Taking into account that ACP transformation into HA need ACP dissolution and renucleation, the achievement of ACP within the CHI hydrogel is indicative of a slowed down rate of dissolution of the amorphous phase, most likely because of the electrostatic adsorption of CHI on the ACP nanoparticles.

In summary, we have prepared ACP/CHI hydrogel nanocomposites (e.g., ACP-NP homogeneously dispersed within CHI hydrogels) by an enzymatically assisted route that causes ACP-NP precipitation and CHI gelation concurrently. ISISA processing of hydrogel nanocomposites allows for the formation of hierarchically organized ACP/CHI materials. Calcination of these materials provides the formation of inorganic hierarchically organized materials (e.g., HA−NP hierarchical structures) in which individual HA nanocrystals aggregate while keeping the macroporous structure. The ISISA process also allows for control of the macroporous size, from 25 up to 90 μm for ACP/CHI hierarchical structures and from 3 up to 9 μm for HA−NP hierarchical structures. The morphology of the resulting hierarchical structures (e.g., microsponge-like) besides the biocompatible chemistry involved in their formation (i.e., combination of an enzymatically assisted route to prepare hydrogel nanocomposite and the ISISA process to create macroporosity) should make these materials very interesting for tissue engineering purposes.

Acknowledgment. This work was supported by CICYT (Project No. MAT2006-02394), Comunidad de Madrid (Project No. S-0505/PPQ-0316). and CSIC (Project Nos. 200660F01 and 200760I009). We also acknowledge TPA Inc. for financial support. M.C.G. acknowledges CSIC for I3P research contract.

Supporting Information Available: Details on experimental procedures for samples preparation and further sample characterization (TG/DTA and DSC experiments, XRD, FTIR spectra, and TEM micrographs; PDF). This material is available free of charge via the Internet at http://pubs.acs.org.

CM7020164

(25) Lévêque, I.; Cusack, M.; Davis, S. A.; Mann, S. *Angew. Chem., Int. Ed.* **2004**, *43*, 885–885.

(26) (a) Tropp, J.; Blumenthal, N. C.; Waugh, J. S *J. Am. Chem. Soc.* **1983**, *105*, 22–26. (b) Aue, W. P.; Roufosse, A. H.; Glimcher, M. J.; Griffin, R. G. *Biochemistry* **1984**, *23*, 6110–6114. (c) Jäger, C.; Welzel, T.; Meyer-Zaika, W.; Epple, M. *Magn. Reson. Chem.* **2006**, *44*, 573–580.